

present computations for the spin parts are considered to be free from the mesonic contributions. In fact, the present systematics obtained for the spin parts of the even-group nucleons indicates that the β -decay matrix elements are insensitive to the mesonic effects, at least for the cases studied here.

In contrast, the orbital parts, especially $\langle \sum \tau_3 l_z \rangle_J$, include possible mesonic contributions. The deviations of $\langle \sum \tau_3 l_z \rangle_J$ from $\langle \sum l_z \rangle_J$ are systematic. In referring to Eq. (5), the deviations are generally the same directions as expected from the mesonic exchange effect (an enhancement of the anomalous moments) which is necessary to account for the magnetic moments of the ^3H - ^3He pair.^{5,6} In this respect, the calculation with configuration mixing alone does not provide the correct

answer as shown by Mavromatis and Zamick⁷ for the magnetic moments of mirror pairs consisting of one particle or one hole beyond a closed major shell.

The spin-orbit force gives rise to a contribution to the effective magnetic moment of a charged particle.⁸ The effect is not charge symmetric. The systematics observed in the spin parts indicates that the contribution is not large enough to affect the results appreciably.

To complete this analysis, further determinations of the magnetic moments of unstable partners of mirror nuclei are highly desirable.

The author would like to thank Dr. M. Morita for discussions and information concerning β decay and Dr. M. Muraoka for discussions.

⁶ R. J. Blin-Stoyle, in *Selected Topics in Nuclear Spectroscopy*, edited by B. J. Verhaar (North-Holland Publishing Co., Amsterdam, 1964), p. 226.

⁷ H. A. Mavromatis and L. Zamick, *Phys. Letters* **20**, 171 (1966).

⁸ J. H. D. Jensen and M. G. Mayer, *Phys. Rev.* **85**, 1040 (1952).

Some Properties of the States at 1.346, 1.459, and 1.554 MeV in $\text{F}^{19}\dagger$

A. R. POLETTI,* J. A. BECKER, AND R. E. McDONALD

Lockheed Palo Alto Research Laboratory, Palo Alto, California 94304

(Received 9 December 1968)

Measurements of the radiative decay of the triplet of levels at 1.346, 1.459, and 1.554 MeV in F^{19} have been made with a $\text{Ge}(\text{Li})$ γ -ray spectrometer. Results of lifetime measurements for these states when averaged with previous work are, respectively, $\tau_m = 4.9 \pm 0.5$ psec, 0.084 ± 0.020 psec, and $4.4_{-2.0}^{+2.4}$ fsec. Accurate energies of the three states were determined to be 1345.75 ± 0.20 , 1459.1 ± 0.5 , and 1554.1 ± 0.3 keV. Information on decay modes and mixing ratios has also been obtained for these states. The decay branching of the 1.459-MeV level was found to differ significantly from that reported by previous investigators. The results are compared with various model predictions.

I. INTRODUCTION

SINCE the pioneering work of Elliott and Flowers¹ and of Redlich,² the structure of the nucleus F^{19} has been the subject of a large number of theoretical investigations. Of particular interest are the works of Harvey,³ Dreizler,⁴ Inoue, Sebe, Hagiwara, and Arima,⁵ Arima, Cohen, Lawson, and Macfarlane,⁶ and Halbert, McGrory, and Wildenthal.⁷ The independent-particle

shell model provided the basis for the investigations of Elliott and Flowers,¹ Redlich,² and Inoue *et al.*⁵ Harvey's description³ of the odd-parity levels within the framework of the SU_3 shell model was successful in describing not only the positions and ordering of the odd-parity levels, but also their major decay properties. Dreizler⁴ employed a core-particle coupling model in which the lowest even-parity states are described in terms of the coupling of a $2s$ - $1d$ hole to the Ne^{20} core. The more recent investigations^{6,7} have involved extensive shell-model calculations. In Ref. 6 the residual nucleon-nucleon interaction for the $(1d_{5/2}, 2s_{1/2})^n$, $n=2-4$, configuration is parameterized in terms of its two-body matrix elements. On the other hand, in Ref. 7 calculations for nuclei with $A=18-22$ are made using a "realistic" effective interaction derived from the Hamada-Johnston potential. In view of the theoretical interest^{7a} in this nucleus and the technical advances in

[†] Work performed at the Lockheed Nuclear Physics Laboratory and at the Stanford University Tandem Van de Graaff Laboratory, supported by the National Science Foundation.

* Present address: Department of Physics, University of Auckland, Auckland, New Zealand.

¹ J. P. Elliott and B. H. Flowers, *Proc. Roy. Soc. (London)* **A229**, 536 (1955).

² M. Redlich, *Phys. Rev.* **99**, 1427 (1955).

³ M. Harvey, *Nucl. Phys.* **52**, 542 (1964).

⁴ R. M. Dreizler, *Phys. Rev.* **136**, B321 (1964).

⁵ T. Inoue, T. Sebe, H. Hagiwara, and A. Arima, *Nucl. Phys.* **59**, 1 (1964).

⁶ A. Arima, S. Cohen, R. D. Lawson, and M. H. Macfarlane, *Nucl. Phys.* **A108**, 94 (1968).

⁷ E. C. Halbert, J. B. McGrory, and B. H. Wildenthal, *Phys. Rev. Letters* **20**, 1112 (1968).

^{7a} Note added in proof: A recent extensive theoretical treatment of the structure of F^{19} is given by H. G. Benson and B. H. Flowers, *Nucl. Phys.* **A126**, 305 (1969).

experimental methods in recent years, it is surprising to find that since the early experimental investigations⁸ of the nuclear structure of the three states at about 1.4 MeV, only a few detailed reinvestigations of the properties of these levels have been reported. One exception is the recent very thorough investigation of the β decay of O^{19} by Olness and Wilkinson.⁹ Short reports have also been published describing Coulomb excitation studies by the Chalk River group¹⁰ and a linear polarization study by Prentice, Gebbie, and Caplan¹¹ which determined the spins and parities of the levels at 1.35 and 1.45 MeV. Booth, Chasan, and Wright¹² have measured the partial widths for the ground-state transitions from the 1459- and 1554-MeV levels. Recently, using the $N^{15}(\alpha, \gamma)F^{19}$ reaction, Tolbert¹³ has measured the lifetime of the 1459-MeV level. In an effort to obtain a more thorough experimental understanding of these levels we have undertaken a series of experiments to investigate their lifetimes, energies, decay modes and the $E2/M1$ mixing ratio of the $1459 \rightarrow 0.110$ transition. A synthesis of the present work with previous measurements is summarized in Fig. 1.

II. EXPERIMENTAL METHOD

The work falls into two parts. An original survey experiment conducted using the Stanford FN tandem accelerator resulted in a firm lifetime for the 1346-keV level, a preliminary value for the lifetime of the 1459-keV level, and a (rather high) upper limit for the lifetime of the 1554-keV level. In subsequent work using the Lockheed 3-MV Van de Graaff accelerator, the attenuated Doppler shifts of the γ rays deexciting the same three levels were studied more thoroughly. As well as this, we measured the angular distributions of the γ rays deexciting the 1459-keV level. Analysis of these latter measurements together with the lifetime determined for this level yielded a value for the $E2/M1$ mixing ratio of the transition from the 1459-keV level to the 110-keV level ($E_\gamma = 1349$ keV). Each set of experiments will now be described.

At Stanford, protons of 5-MeV energy were used to bombard a 1-mg/cm²-thick SrF_2 target which had been evaporated onto a tantalum backing. Gamma radiation from the resulting $F^{19}(p, p')F^{19*}$ reaction was detected using a 20-cm³ Ge(Li) detector which could be placed to view γ rays emitted from the target at either $\theta_\gamma = 0^\circ$ or 90° with respect to the beam direction. Amplified pulses from the detector were digitized using one-half of a Northern Scientific dual 4096-channel

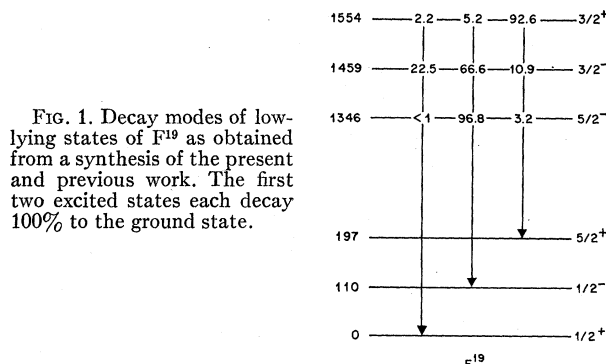


FIG. 1. Decay modes of low-lying states of F^{19} as obtained from a synthesis of the present and previous work. The first two excited states each decay 100% to the ground state.

analog-to-digital converter (ADC) interfaced to a Digital Equipment Corporation PDP-7 computer equipped with 8192 words of memory. The spectra were stored in the memory as a 4096-channel array with the aid of a general Dual ADC program written by Dr. P. R. Bevington, Stanford.¹⁴ Spectra were recorded in a series of four runs taken alternately with $\theta_\gamma = 0^\circ$ and 90° , with calibration spectra recorded before and after. The gain of the γ -ray spectrometer was not stabilized but remained stable to better than a channel in 4000 throughout the entire experiment.

A more comprehensive program was undertaken at Lockheed: The experimental method was essentially the same as at Stanford except that now the Ge(Li) detector could be set at any angle θ_γ between 0° and 90° with respect to the incident beam direction. In the first series of experiments, conducted at a bombarding energy of 2.80 MeV, we used a thin target of CaF_2 (40 $\mu\text{g}/\text{cm}^2$ thick) evaporated onto a tantalum backing. Spectra were recorded in random order at angles of 0° (thrice), 30° , 45° , 60° , and 90° (thrice). In a second series, at an incident bombarding energy of 2.89 MeV, thin CaF_2 targets (40 $\mu\text{g}/\text{cm}^2$) were mounted alternately so that the fluorine ions recoiled either into vacuum or into a tantalum stopper. Spectra were recorded with $\theta_\gamma = 0^\circ$ except for one measurement at $\theta_\gamma = 90^\circ$, which was used to determine the unshifted energy of the observed γ rays. A third series involved the detection of γ rays from a thin CaF_2 target deposited on a calcium foil. The object of this series was to provide a stopping material with a relatively long characteristic slowing down time in order to obtain a more accurate value of the long-lived (≈ 5 psec) 1346-keV level. Unfortunately, although the calcium foil had appeared to be unoxidized when the CaF_2 was deposited on it, later analyses indicated a characteristic stopping time which was much faster than expected for pure calcium. Evidently, a substantial oxidation of the surface layer (≈ 200 $\mu\text{g}/\text{cm}^2$) had indeed taken place. In this and the preceding series the gain of the γ -ray spectrometer was continuously monitored by placing a Co^{60} source near the detector. The amplified pulses from the Ge(Li) detector were digitized using a

⁸ B. J. Toppel, D. H. Wilkinson, and D. E. Alburger, Phys. Rev. **101**, 1485 (1956).

⁹ J. W. Olness and D. H. Wilkinson, Phys. Rev. **141**, 966 (1966).

¹⁰ A. E. Litherland, M. A. Clark, and C. Broude, Phys. Letters **3**, 204 (1963).

¹¹ J. D. Prentice, N. W. Gebbie, and H. S. Caplan, Phys. Letters **3**, 201 (1963).

¹² E. C. Booth, B. Chasan, and K. A. Wright, Nucl. Phys. **57**, 403 (1964); E. C. Booth and K. A. Wright, *ibid.* **35**, 472 (1962).

¹³ D. D. Tolbert, University of Kansas (unpublished).

¹⁴ P. R. Bevington (private communication).

TABLE I. Gamma rays from excited states of F^{19} as measured in the present work.

γ -ray energy (keV)	Level assignment (keV)
1235.9 ± 0.2	$1346 \rightarrow 110$
1261.6 ± 0.3	$1459 \rightarrow 197$
1348.9 ± 0.3	$1459 \rightarrow 110$
1356.9 ± 0.4	$1554 \rightarrow 197$
1444.5 ± 0.7	$1554 \rightarrow 110$
1458.9 ± 0.4	$1459 \rightarrow 0$
1554.9 ± 1.0	$1554 \rightarrow 0$

Nuclear Data Dual 4096-channel ADC interfaced to a Systems Engineering Laboratories SEL 810A computer equipped with 8192 words of memory. Data were again stored as 4096-channel arrays in computer memory using a data-acquisition program written by R. A. Chalmers, Lockheed.¹⁵

In both sets of experiments described above the data were recorded on magnetic tape. This tape could then be read into a Univac 1108 computer for subsequent off-line analysis which included plotting, calculation of centroids and areas of peaks, calibration of spectra, and fitting of angular distributions.

Doppler-shift attenuation measurements of nuclear lifetimes using Ge(Li) detectors have been described in a number of recent works.^{16,17} At this point we will merely reiterate some salient features relevant to the present work. For the range of F^{19} recoil velocities which we used ($v/v_0 \leq 0.7$, where $v_0 = c/137$) it is sufficient⁷ to approximate the slowing-down process by

$$-M_1(dv_z/dt) = K_e v_z/v_0 + K_n (v_z/v_0)^{-1}.$$

Here M_1 denotes the mass of the ion being stopped, v_z is its velocity in the z direction, while K_e and K_n are the proportionality constants for energy loss by electronic and nuclear collisions, respectively. For K_e we took the Lindhard-Scharff estimate.¹⁸ There is evidence¹⁹ that for stopping in carbon this figure should be increased by 29% while for stopping in aluminum the corresponding figure is 10%. It is difficult to extrapolate this trend with any certainty to the stopping materials

¹⁵ R. A. Chalmers (private communication).

¹⁶ A. E. Litherland, M. J. L. Yates, B. M. Hinds, and D. Eccleshall, Nucl. Phys. **44**, 220 (1963); J. W. Olness and E. K. Warburton, Phys. Rev. **151**, 792 (1966); E. K. Warburton, D. E. Alburger, and D. H. Wilkinson, *ibid.* **129**, 2180 (1963); E. K. Warburton, J. W. Olness, K. W. Jones, C. Chasman, R. A. Ristinen, and D. H. Wilkinson, *ibid.* **148**, 1072 (1966).

¹⁷ E. K. Warburton, J. W. Olness, and A. R. Poletti, Phys. Rev. **160**, 938 (1967).

¹⁸ J. Lindhard, M. Scharff, and H. E. Schiott, Kgl. Danske Videnskab. Selskab, Mat.-Fys. Medd. **33**, No. 14 (1963); J. Lindhard and M. Scharff, Phys. Rev. **124**, 128 (1961).

¹⁹ J. H. Ormrod, J. R. MacDonald, and H. E. Duckworth, Can. J. Phys. **43**, 275 (1965).

used in the present work (Ta and SrF_2); therefore the Lindhard-Scharff¹⁸ estimates, $K_e = 0.594 \text{ keV cm}^2/\mu\text{g}$ (F^{19} in Ta) and $K_e = 1.575 \text{ keV cm}^2/\mu\text{g}$ (F^{19} in SrF_2) were used. We estimated K_n following the procedure as outlined by Warburton *et al.*,¹⁷ resulting in $K_n = 0.091 \text{ keV cm}^2/\mu\text{g}$ (F^{19} in Ta) and $K_n = 0.171 \text{ keV cm}^2/\mu\text{g}$ (F^{19} in SrF_2). With the above estimates, Eq. (B15) of Ref. 17 gives the dependence of $F(\tau) = \Delta E_{\text{stop}}/\Delta E_{f.s.}$, upon the nuclear lifetime. ΔE_{stop} is the measured energy shift in going from detection at 90° to detection at 0° with the F^{19} ions recoiling into a stopping medium while $\Delta E_{f.s.}$ is the expected full shift under the same circumstances. We determined $\Delta E_{f.s.}$ either by calculation from the known kinematics of the reaction or by direct measurement when the F^{19} ions were allowed to recoil into a vacuum. If $F(\tau)$ is close to zero, alternate measurements at 0° and 90° yield the best estimate of $F(\tau)$; while if $F(\tau)$ is close to unity, measurements at 0° with the F^{19} recoiling alternately into a stopping medium or vacuum will give the best estimate. Depending on the lifetime, we used both methods. A numerical integration of Eq. (B15) in Ref. 17, done using a code due to Warburton *et al.*,¹⁷ enabled us to extract either mean lifetimes (τ_m) or limits from the measured values of $F(\tau)$.

III. EXPERIMENTAL RESULTS

Table I lists the energies, as measured in the present study, of seven of the primary γ rays originating from the three levels of interest. Except for the γ rays originating from the 1459-keV level, these are in good agreement with the measurement reported in Ref. 17 or the γ -ray energies implied by the listed level energies

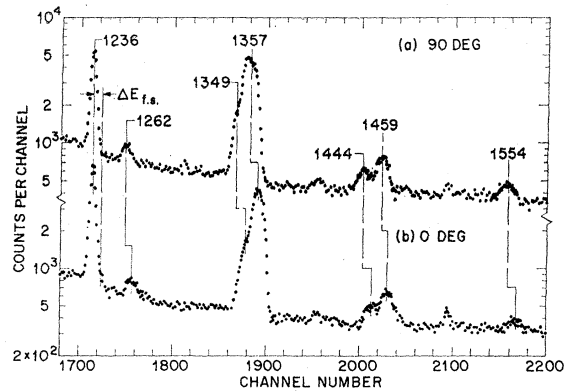


FIG. 2. Partial spectra obtained using a Ge(Li) γ -ray detector to observe γ rays resulting from bombardment with 5-MeV protons of a 1-mg/cm² SrF_2 target evaporated on to a tantalum backing. The upper spectrum (a) was obtained by detecting γ rays emitted from the target at 90° with respect to the beam direction. The lower spectrum corresponds to the observation of γ rays emitted at 0° with respect to the beam. The effect of the small Doppler shifting of the 1236-keV γ ray can be discerned as a small high-energy tail in the 0° spectrum. The full-energy γ -ray peaks, labeled by their energy in keV, all arise from the radiative decay of bound states in F^{19} . Table I lists the accurate γ -ray energies together with their assignments.

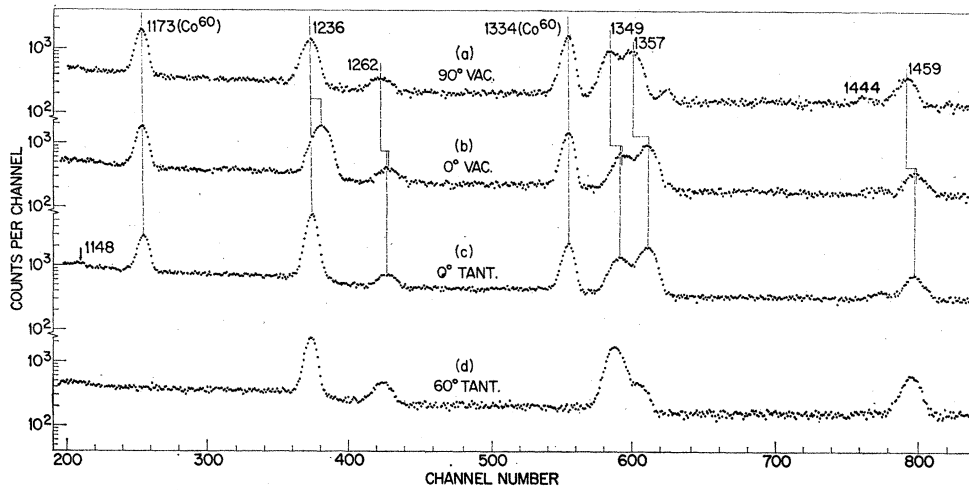


FIG. 3. Partial spectra obtained using a Ge(Li) γ -ray detector to observe γ rays resulting from the bombardment of a $40\text{-}\mu\text{g}/\text{cm}^2$ CaF_2 target by protons of either 2.89 MeV (upper spectra) or 2.80 MeV (lowest spectrum). The uppermost spectrum (a) corresponds to the detection of γ rays emitted at 90° with respect to the beam direction. Spectra (b) and (c) correspond to the detection of γ rays emitted at 0° with respect to the beam direction and to the F^{19} ions recoiling, respectively, into vacuum and into a tantalum stopper. Gamma-ray peaks arising from the decay of levels in F^{19} are labeled by their energy in keV (see Table I). For the 1357-keV γ ray corresponding to the major decay of the 1554-keV level in F^{19} there was no detectable difference between the energies as determined from spectrum (b) and spectrum (c). For the γ rays corresponding to the decay of the 1459-keV level in F^{19} , however, there was a definite attenuation of the full Doppler shift: $F(\tau) = 0.89 \pm 0.05$. Spectrum (d) recorded at a detection angle of 60° [$P_2(\cos\theta)$ is small at this angle] is included to illustrate our reason for revising the commonly accepted branchings of the 1459-keV level. The areas of the peaks at 1262, 1349, and 1459 keV are in the ratio 11.1:68.5:20.3. This ratio when corrected for the slight differences in the detection efficiency for the different γ -ray energies is very close to the values quoted in Table III. The latter values were obtained from the A_θ coefficients of the angular-distribution measurements.

of Spilling *et al.*²⁰ Listed in Table II are the level energies which we derived from the γ -ray energies presented in Table I. The last column of this table gives the energies which we adopt for the first five excited states on the basis of this and previous work. From an analysis of the areas of the different γ -ray peaks in various spectra (see, for example, Figs. 2 and 3) and from measurements of the relative efficiency of the γ -ray spectrometer, we determined the decay modes listed in Table III. Our results for the 1554-keV level are in good agreement with the recent measurement of Olness and Wilkinson⁹ while, except for the occurrence of a γ ray

of 1148 keV which we assign to a definite $(3.2 \pm 1)\%$ branch from the 1346-keV level to the 197-keV level, we agree with previous determinations²¹ of the decay modes of the 1346-keV level. Our results for the decay of the 1459-keV level are not, however, in agreement

TABLE II. Energies of excited states in F^{19} .

State	Present	Energy (keV) Previous	Adopted
1		109.894 ± 0.0005^a	109.894 ± 0.005
2	197.6 ± 0.6	197.2 ± 0.2^b	197.3 ± 0.2
3	1345.8 ± 0.2	1345.7 ± 0.2^c	1345.75 ± 0.2
4	1459.1 ± 0.5	1456.9 ± 1.1^b	1459.1 ± 0.5
5	1554.2 ± 0.4	1554.0 ± 0.3^b	1554.1 ± 0.3

^a E. J. Seppi and F. Boehm, Phys. Rev. **128**, 2334 (1962).

^b Reference 20.

^c Reference 17.

²⁰ P. Spilling, H. Gruppelaar, H. F. DeVries, and A. M. J. Spits, Nucl. Phys. **A113**, 395 (1968).

TABLE III. Decay modes of low-lying levels of F^{19} .

Initial level keV (J^π)	Final-level (transition energy) in (keV)	Branching (%)		
		This work	Previous	Adopted
1346($\frac{5}{2}^-$)	0(1346)	<1	<5 ^a	<1
	110(1236)	96.8 ± 1	100 ^a	96.8 ± 1
	197(1149)	3.2 ± 1	<6 ^a	3.2 ± 1
1459($\frac{3}{2}^-$)	0(1459)	22.5 ± 2	15 ^b	22.5 ± 2
	110(1349)	66.6 ± 3	85 ^b	66.6 ± 3
	197(1262)	10.9 ± 2	<6 ^b	10.9 ± 2
1554($\frac{3}{2}^+$)	0(1554)	2.0 ± 0.7	2.4 ± 0.5^c	2.2 ± 0.5
	110(1444)	5.3 ± 1	5.2 ± 0.7^c	5.2 ± 0.7
	197(1357)	92.7 ± 1	92.4 ± 0.9^c	92.6 ± 0.9

^a Reference 21.

^b References 8 and 22.

^c Reference 9.

²¹ F. Ajzenberg-Selove and T. Lauritsen, Nucl. Phys. **11**, 1 (1959).

TABLE IV. Results of lifetime measurements in F^{19} from the present work.

Level (keV)	Bombarding energy (MeV)	Stopper	$F(\tau)$	τ (psec)
1345.8	5.00	SrF ₂	0.05 ± 0.01	$5.3_{-0.9}^{+1.5}$
1459.1	2.89	Ta	0.82 ± 0.08	0.057 ± 0.024
1554.1	2.89	Ta	1.02 ± 0.04	< 0.017

with previous measurements.^{8,22} Figure 3(d) is an illustration of the type of data upon which we base our conclusions. We obtain substantially higher branchings for the decay of the 1459-keV level to both the ground state and the 197-keV level than those reported earlier.⁸ Because the Ge(Li) detector which we used has a much higher γ -ray resolution than the NaI(Tl) detectors employed previously,^{8,22} we adopt for this level the branchings measured in the present work.

The lifetime of the 1346-keV level which we quote in Table IV was obtained from an analysis of the data recorded during the Stanford experiments (Fig. 2). Only a slight shift of the centroid of the 1236-keV γ ray was observed when the γ -ray detector angle was changed from $\theta_\gamma = 0^\circ$ to $\theta_\gamma = 90^\circ$: $\Delta E = 0.29 \pm 0.06$ keV. This implies $F(\tau) = 0.05 \pm 0.01$ and $\tau_m = 5.3_{-0.9}^{+1.5}$ psec. This value is in good agreement with two recent meas-

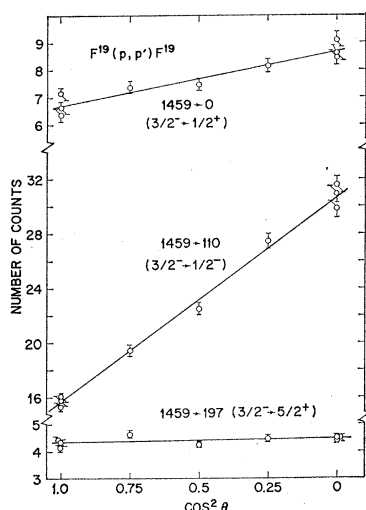


FIG. 4. The measured angular distributions of γ rays de-exciting the F^{19} 1459-keV level. The pronounced anisotropy of the 1459 keV \rightarrow 110 keV transition immediately indicates that the phase of the mixing ratio for this transition is positive. The angular distribution of the 1459 keV \rightarrow 197 keV transition is nearly isotropic, as expected, for a primarily dipole $\frac{3}{2} \rightarrow \frac{5}{2}$ transition.

²² C. M. P. Johnson, G. A. Jones, W. R. Phillips, and D. H. Wilkinson, Proc. Roy. Soc. (London) A252, 1 (1959).

urements: $\tau_m = 5.2 \pm 0.9$ ²³ and 4.7 ± 0.6 psec.²⁴ We adopt the value $\tau_m = 4.9 \pm 0.5$ psec for the purposes of further discussion. In addition, Fig. 2 shows very clearly the three decay modes of the 1554-keV level. These correspond to the peaks labeled 1357, 1444, and 1554 keV in the figure. Both the lifetime measurement for the 1459-keV level and the upper limit on the lifetime of the 1554-keV level were obtained from an analysis of spectra such as those displayed in Fig. 3. For the γ rays originating directly from the 1459-keV level, a comparison between the centroid energies measured with $\theta_\gamma = 0^\circ$ for the two cases of F^{19} recoiling into vacuum and recoiling into a tantalum stopper resulted in a value of $F(\tau) = 0.82 \pm 0.08$, which implies a lifetime $\tau_m = 0.057 \pm 0.024$ psec. This is in reasonable agreement with the

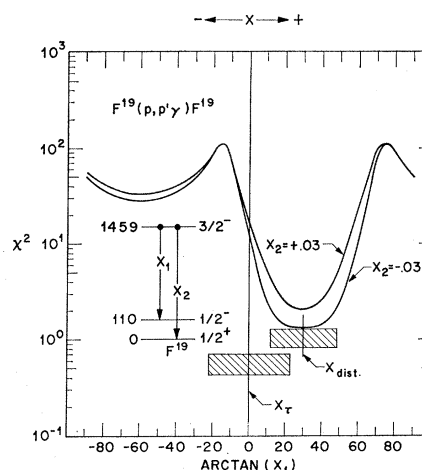


FIG. 5. Plot of χ^2 versus $\arctan x_1$ for a simultaneous fitting of the two transitions indicated in the insert. The mixing ratio x_2 was allowed to vary over the region allowed by the lifetime data: $|x_2| < 0.03$. There is one broad solution: $x_1 = 0.58_{-0.37}^{+0.53}$. See text for details.

resonance-fluorescence results^{12,25} of 0.093 ± 0.030 and 0.075 ± 0.023 psec and Tolbert's recent measurement¹³ of 0.102 ± 0.035 psec. Table IV shows the values obtained for the lifetimes measured in the present work. In Table V, we average the present results with these previous measurements and adopt the value 0.084 ± 0.020 psec for the purposes of further discussion.

For the major decay from the 1554-keV level, no significant difference between the vacuum shift [Fig. 3(b)] and that obtained when the F^{19} recoils were being stopped in tantalum [Fig. 3(a)] was observed:

$$F(\tau) = 1.02 \pm 0.04,$$

²³ P. Paul, J. W. Olness, and E. K. Warburton, Phys. Rev. 173, 1063 (1968).

²⁴ K. W. Jones, A. Z. Schwartzschild, E. K. Warburton, and D. B. Fossan, Phys. Rev. 178, 1773 (1969).

²⁵ The lifetimes quoted in Ref. 12 have been corrected to take account of the decay modes adopted in Table III.

TABLE V. Lifetimes of excited states in F^{19} .

Level (keV)	Present	Lifetime Previous	Adopted
1345.8	$5.3_{-0.9}^{+1.5}$ psec	5.2 ± 0.9 psec ^a 4.7 ± 0.6 psec ^b	4.9 ± 0.5 psec
1459.1	0.057 ± 0.024 psec	0.093 ± 0.030 psec ^c 0.075 ± 0.023 psec ^c 0.102 ± 0.035 psec ^d	0.084 ± 0.020 psec
1554.1	< 17 fsec	$4.4_{-2.0}^{+2.4}$ fsec ^e	$4.4_{-2.0}^{+2.4}$ fsec

^a Reference 23.^b Reference 24.^c Reference 12.^d Reference 13.^e This lifetime is derived from the partial width quoted in Ref. 12 and the adopted decay modes of Table III.

that is,

$$\tau_m \leq 17 \text{ fsec.}$$

This is in agreement with, but not as useful, as the lifetime $\tau_m = 4.4_{-2.0}^{+2.4}$ fsec for this level which can be derived from a synthesis of the partial lifetime quoted by Booth *et al.*¹² and the branchings quoted in Table III.

The angular distribution of the γ rays deexciting the 1459-keV level are displayed in Fig. 4, while Table VI lists the Legendre coefficients obtained from a least-squares fit to the experimental data. The adopted lifetime (0.084 ± 0.020 psec) together with the decay modes given in Table III and an allowance of a maximum enhancement of 4 Weisskopf units²⁶ for the possible $M2$ component in the 1459-keV γ ray limits the mixing ratio for this transition to $|x_2| < 0.03$. The mixing ratio of the 1459 \rightarrow 197 transition is similarly

limited to the region $|x| < 0.03$. The angular distribution of this transition can therefore be used to determine the alignment of the 1459-keV level at the bombarding energy of 2.80 MeV.²⁷ A simultaneous fit of the 1459 \rightarrow 0 and 1459 \rightarrow 110 transitions as a function of the mixing ratio (x_1) of the 1459 \rightarrow 110 transition therefore yields in general two allowed regions for x_1 . In this particular case, however, the two solutions coalesce, resulting in one rather broad allowed region, $x_1 = 0.58_{-0.37}^{+0.53}$, as illustrated in Fig. 5. The overlap between this allowed region and the region permitted by the known lifetime [allowing a maximum enhancement of 81 Weisskopf units (Z^2) for the $E2$ component of the 1459 \rightarrow 110 transition] implies a mixing ratio

TABLE VI. Angular distributions of γ rays observed following inelastic proton scattering from F^{19} at a bombarding energy of 2.80 MeV.

Energy (keV)	Transition	A_2/A_0	A_4/A_0	χ^2
1236	1346 \rightarrow 110	0.374 ± 0.012	-0.022 ± 0.016	0.54
1262	1459 \rightarrow 197	-0.015 ± 0.017	-0.007 ± 0.021	1.47
1349	1459 \rightarrow 110	-0.396 ± 0.013	$+0.010 \pm 0.013$	1.67
1459	1459 \rightarrow 0	-0.167 ± 0.019	$+0.008 \pm 0.022$	2.10

TABLE VII. Mixing ratios of some transitions in F^{19} .

Transition	Mixing ratio	Source
1554 \rightarrow 0	$ x = 0.25 \pm 0.06$	a, b
\rightarrow 110	$ x \leq 0.016$	c, ($ M(M2) ^2 \leq 2$)
\rightarrow 197	$ x \leq 0.10$	c, ($ M(E2) ^2 \leq 81$)
1459 \rightarrow 0	$ x \leq 0.03$	c, ($ M(M2) ^2 \leq 4$)
\rightarrow 110	$x = +0.27 \pm 0.10$	c, d
\rightarrow 197	$ x \leq 0.03$	c, ($ M(M2) ^2 \leq 4$)

^a Reference 10.^b Reference 12.^c Present work. The transition strengths are in Weisskopf units (Ref. 26).^d Reference 11.

²⁶ D. H. Wilkinson, in *Nuclear Spectroscopy*, edited by F. Ajzenberg-Selove (Academic Press Inc., New York, 1960), Part B, pp. 862 ff.

²⁷ H. J. Rose and D. M. Brink, *Rev. Mod. Phys.* **39**, 306 (1967); A. R. Poletti and E. K. Warburton, *Phys. Rev.* **137**, B595 (1965).

TABLE VIII. Comparison of experimental partial widths with some theoretical predictions. Columns 2 and 3 give the experimentally determined partial widths in meV for the transitions indicated in column 1. Columns 4 and 5 give the same quantity in terms of Weisskopf units. Various theoretical predictions are compared with these measurements in the last two columns. For the purposes of quoting partial widths in Weisskopf units, positive and negative quoted errors have sometimes been equalized.

Transition	Partial width (meV)		Partial width (Weisskopf units)		
	Dipole	Quadrupole	Dipole	Quadrupole	Other Dreizler ^a (Dip, Quad)
1554→0(<i>M1</i> / <i>E2</i>)	3.1 _{-1.1} ^{+2.6}	0.20±0.07 ^b	0.05±0.02	9±3	10 ⁻³ , 9
110(<i>E1</i> / <i>M2</i>)	7.6 _{-2.8} ^{+6.5}	<3.7×10 ⁻³	(6.6±3.2)×10 ⁻³	<4	0.004, 5.72 ^c
197(<i>M1</i> / <i>E2</i>)	(1.4 _{-0.5} ^{+1.2})×10 ²	<2.6	3.3±1.5	d	1.84, 5.5
1459→0(<i>E1</i> / <i>M2</i>)	1.8 _{-0.4} ^{+0.9}	<2.3×10 ⁻³	(1.3±0.4)×10 ⁻³	<3.4	2.16, 2.6 ^c
110(<i>M1</i> / <i>E2</i>)	4.9 _{-1.2} ^{+2.3}	0.34 _{-0.17} ^{+0.34}	0.10±0.03	31±16	1.2, ...
197(<i>E1</i> / <i>M2</i>)	0.9 _{-0.2} ^{+0.4}	<1.2×10 ⁻³	(0.9±0.3)×10 ⁻³	<3.4	0.22, 23.77 ^c
1346→0(<i>M2</i>)	...	<1.5×10 ⁻³	<4	<4	...
110(<i>E2</i>)	...	(13.5±1.4)×10 ⁻²	19.2±1.7
197(<i>E1</i> / <i>M2</i>)	<4.8×10 ⁻³	<8×10 ⁻⁴	<6.6×10 ⁻⁴	<4	...

^a Reference 4.

^b Reference 10.

^c J. B. McGroarty (private communication) quotes the following widths (meV): $\Gamma_{M1}(\frac{3}{2} \rightarrow \frac{1}{2}) = 113.8$.

$\Gamma_{M1}(\frac{3}{2} \rightarrow \frac{1}{2}) = 0.3$, $\Gamma_{E2}(\frac{3}{2} \rightarrow \frac{1}{2}) = 0.03$, $\Gamma_{E2}(\frac{3}{2} \rightarrow \frac{1}{2}) = 0.13$. See also Ref. 7.
^d For purposes of computation we have assumed $|M(E2)|^2 < 81$.
^e Reference 3.

+0.21≤*x*₁≤+0.50. The phase convention used in quoting this result is that of Rose and Brink.²⁷ Prentice *et al.*'s value¹¹ for this mixing ratio is, using the same sign convention, *x*₁=+0.23±0.10. We adopt an average value *x*₁=+0.27±0.10.

IV. DISCUSSION

Information previously available on the lifetimes of each level has been combined with that obtained in the present work and is presented in Table V. In addition to this it is possible to obtain further information on the possible dipole/quadrupole mixing ratios. This information is presented in Table VII and is used together with the lifetimes to arrive at the results presented in Table VIII for most of the possible dipole or quadrupole transitions from the triplet of levels. The most striking thing about this table is the pronounced inhibition of the four *E1* transitions. Harvey³ has shown that this inhibition can be understood on the basis of the *SU*₃ model of the low-lying states of F¹⁹. On this model all *E1* transitions are zero. This is because in the model³ the c.m. of the proton group in both positive- and negative-parity states is in an *S* state.

Table VIII also shows the great differences in the strength of the two *M1* transitions from the 1554-keV level. This was one of the major successes of Elliott and Flower's original paper¹ and has a simple explanation. In the shell-model L-S expansion both the 1.554- and the 0.197-MeV states have the *d*³ and *ds*² configurations as their major component while the ground state is predominantly *d*²*s* and *s*³. Since there can be no *M1* transitions between these two sets of configurations (*d*³, *ds*²)→(*d*²*s*, *s*³), the ground-state transition is greatly hindered. Harvey's *SU*₃ model is also successful at explaining the somewhat retarded *M1* transition between the $\frac{3}{2}^-$ and $\frac{1}{2}^-$ states, and the greatly enhanced *E2* transitions from the $\frac{3}{2}^-$ and $\frac{5}{2}^-$ states to the $\frac{1}{2}^-$ state. The weak-coupling model also illuminates these transitions between the various members of the odd-parity band. This model describes the $\frac{3}{2}^-$ and $\frac{5}{2}^-$ states as a *p*_{1/2} hole coupled to the 2⁺ first excited state of Ne²⁰. In the same spirit the $\frac{1}{2}^-$ state at 110 keV is described as a *p*_{1/2} hole coupled to the Ne²⁰ ground state. On the basis of this model, the *M1*($\frac{3}{2}^- \rightarrow \frac{1}{2}^-$) transition is forbidden while the strength of the *E2* transitions ($\frac{3}{2}^- \rightarrow \frac{1}{2}^-$) and ($\frac{5}{2}^- \rightarrow \frac{1}{2}^-$) should be equal to that of the Ne²⁰ 1.63-MeV (2⁺→0⁺) transition. For the *E2* transitions this is indeed so, the transition strengths in Weisskopf units²⁵ being, respectively, $|M(E2)|^2 = 19.2 \pm 1.7$, 31±16, and 23.06±3.7.

ACKNOWLEDGMENT

We would like to express our thanks to all the members of the Stanford FN Tandem Group for their helpfulness.